GEOLOGY | THE GEOLOGICAL SOCIETY OF AMERICA®

https://doi.org/10.1130/G47579.1

Manuscript received 4 March 2020
Revised manuscript received 22 April 2020
Manuscript accepted 23 April 2020

Published online 5 June 2020

Noble metal nanonugget insolubility in geological sulfide liquids

Michael Anenburg and John A. Mavrogenes
Research School of Earth Sciences, Australian National University, Canberra, Australian Capital Territory 2600, Australia

ABSTRACT

Noble metals (NMs) in Earth's magmatic systems are thought to be controlled entirely by their strong partitioning to sulfide liquids. This chemical equilibrium is at the root of various models, ranging from NM deposit formation to planetary differentiation. Noble metals commonly occur as sub-micrometer phases known as nanonuggets. However, the assumptions that nanometer-scale thermodynamic equilibrium partitioning is attained and that NM nanonuggets are soluble in sulfide liquids have never been validated. Using novel experimental methods and analytical techniques we show nanometer-scale NM ± Bi phases attached to exterior surfaces of sulfide liquids. Larger phases (≤1 µm) show clear liquid immiscibility textures, in which Fe, Cu, and Ni partition into sulfide liquids whereas NMs partition into bismuthide liquids. Noble metal compositions of sulfides and their associated NM phases vary between adjacent droplets, indicating NM disequilibrium in the system as a whole. We interpret most nanometer-scale NMs contained within sulfides to be insoluble as well, suggesting that previously reported sulfide–silicate partition coefficients are overestimated. Consequently, sulfide liquids likely play a secondary role in the formation of some NM ore deposits.

INTRODUCTION

The noble metals (NMs, consisting of Au, Ag, and the platinum group elements [PGEs]: Ru, Rh, Pd, Os, Ir, and Pt) have important economic, industrial, social, and scientific applications (Gunn, 2014). In addition, these metals are used as tracers of planetary evolution, on Earth and elsewhere in the solar system (Day et al., 2016; Luguet and Reisberg, 2016). The geochemistry of NMs is considered to be dominated by their strong affinities to sulfide. Reported equilibrium partition coefficients for the PGEs between conjugate sulfide and silicate liquids range in the thousands to millions, with the practical implications that sulfide liquids completely strip coexisting silicate melts of NMs and dissolve them in their entirety in a homogenous sulfide liquid (Sattari et al., 2002; Mungall and Brenan, 2014; Laurenz et al., 2016). Indeed, NMs most commonly occur associated with base-metal sulfides, an association commonly explained by crystallization of the NMs directly from the sulfide liquid, or as later solid-state exsolution from sulfide minerals (Holwell and McDonald, 2010; Godel, 2015). In PGE ore deposits, equilibrium partitioning of PGEs into sulfide melt and subsequent crystallization have been used to explain their concentration, using the R-factor equation (Campbell and Naldrett, 1979), which accounts for the NMs deposited relative to the volume of silicate melt from which it was extracted. In these deposits, PGEs occur as platinum group minerals (PGMs), which consist of one or more PGEs as a major element, commonly bonded with sulfur or the semi-metals Te, As, Bi, Sn, and Sb (TABS).

Equilibrium partitioning models have explained many features of PGE deposits, but some unresolved issues remain. First, PGMs are not always contained within sulfides, occurring either at grain boundaries or associated with silicates or oxides (Godel et al., 2010). Second, PGM assemblages and compositions vary between nearby sulfides, indicating disequilibrium on the micrometer to centimeter scale. Finally, some ore deposits paradoxically contain more PGEs than could have been dissolved in the entire magma chamber, and do not contain enough sulfur to account for the observed PGE budget (Naldrett et al., 2009). These discrepancies are commonly explained by later sulfur loss or low-temperature alteration, but not without controversy because evidence for these processes is often inconclusive (Godel et al., 2010; Barnes and Ripley, 2016; Kawohl and Frimmel, 2016).

Crystallization of PGMs directly from sulfur-undersaturated silicate melts has been suggested (Spandler et al., 2000; Finnigan et al., 2008; Maier et al., 2015; Anenburg and Mavrogenes, 2016), but not for the most common PGE-bearing sulfide-saturated magmatic systems. PGEs distributed in experimental silicate melts as "nanonuggets" (sub-micrometer phases) are commonly interpreted as experimental artifacts and thus disregarded. Recent observations of natural quenched sulfides containing random PGE nanonugget distributions argue against the traditional equilibrium partitioning model (Zelenski et al., 2017; González-Jiménez et al., 2019; Kamenetsky and Zelenski, 2020). Additionally, primitive sulfide melts described by Savelyev et al. (2018) show order-of-magnitude variabilities between adjacent sulfide melts. Nonetheless, the accepted mainstream view is one of PGE crystallization out of initially homogenous equilibrated sulfide liquids (Holwell and McDonald, 2010; Godel, 2015).

Experimental studies of NM-sulfide-silicate systems are challenging because silicate melts are commonly sealed within PGE capsules, which contribute unrealistically high NM contents. Furthermore, NM capsules are incompatible with sulfides, which react to compromise experiments and their results. Finally, consistent control of oxygen fugacity is critical for maintaining reproducible PGE solubility and sulfur speciation results. In this study, we use a novel experimental setup that allows us to study sulfides, silicates, and PGEs simultaneously. We ran piston-cylinder experiments in which layers of nanonugget-bearing, NM-Bi-enriched oxidized silicate glass, synthetic chromite (guided by the NM-chromite association in nature), and Fe-Cu-Ni sulfides were run inside a graphite capsule within a sealed nickel capsule at 5 kbar and 1100 °C. Three experiments are reported here. Experiments D2905 and D2909 ran for 4 h, and experiment C5774 ran for 17 h. Oxygen fugacity (f_{O_2}) was buffered at the C-CO-CO_2 redox buffer (CCO) by the coexistence of graphite and CO_2 generated by in situ reduction of the oxidized

CITATION: Anenburg, M., and Mavrogenes, J.A., 2020, Noble metal nanonugget insolubility in geological sulfide liquids: Geology, v. 48, p. 939–943, https://doi.org/10.1130/G47579.1

starting materials. At our conditions, CCO is roughly one log f_{O_2} unit lower than the fayalite-magnetite-quartz buffer. Detailed methods are available in the Supplemental Material[1].

RESULTS

Experiments quenched to homogenous silicate glass containing crystals of clinopyroxene and chromite, and sulfide droplets. The clinopyroxene and chromite did not affect the sulfide or NM relationships and will not be discussed further. We find abundant NM nanonuggets on external surfaces of the sulfide droplets (Figs. 1A and 1B), and fewer inside sulfide droplets (Figs. 1C and 1D). Large NM-Bi blebs (~1 µm) appear immiscible with the sulfide droplets they are in contact with. The base metals Fe, Ni, and Cu occur in the sulfide phase, whereas the NMs are present in the immiscible bismuthide melt (Figs. 1E and 1F). The NM contents of hybrid sulfide-bismuthide droplets contain variable combinations of NMs and Bi (Figs. 1 and 2). For example, Figure 2A shows a droplet (marked by the black arrow) that lacks Pt and Ir, while Ru appears above the actual droplet. Another droplet (Fig. 2B) lacks Ru and Rh, while Ag occurs below as well as within the droplet. The droplet in Figure 2C differs by containing Ir but no Ag, Pd, or Au, which were present in the previous droplets. Likewise, all droplets shown in Figures 2D–2F contain a seemingly random combination of NMs. Some nanonuggets are not associated with sulfides or bismuthides, but appear isolated in the silicate glass (white arrows in Fig. 2). A remarkable example is shown in Figure 2D, where a sulfide-bismuthide droplet contains Rh and Au, whereas all other PGEs (Pt, Ir, Rh, and Ru) occur as nanonuggets in close proximity (<~5 µm) to the droplet but not in actual contact.

[1]Supplemental Material. Detailed experimental and analytical methods, high-resolution versions of Figures 1 and 2, and the LA-ICP-MS data set including the R code used to generate Figure 2. Please visit https://doi.org/10.1130/GEOL.S.12360560 to access the supplemental material, and contact editing@geosociety.org with any questions.

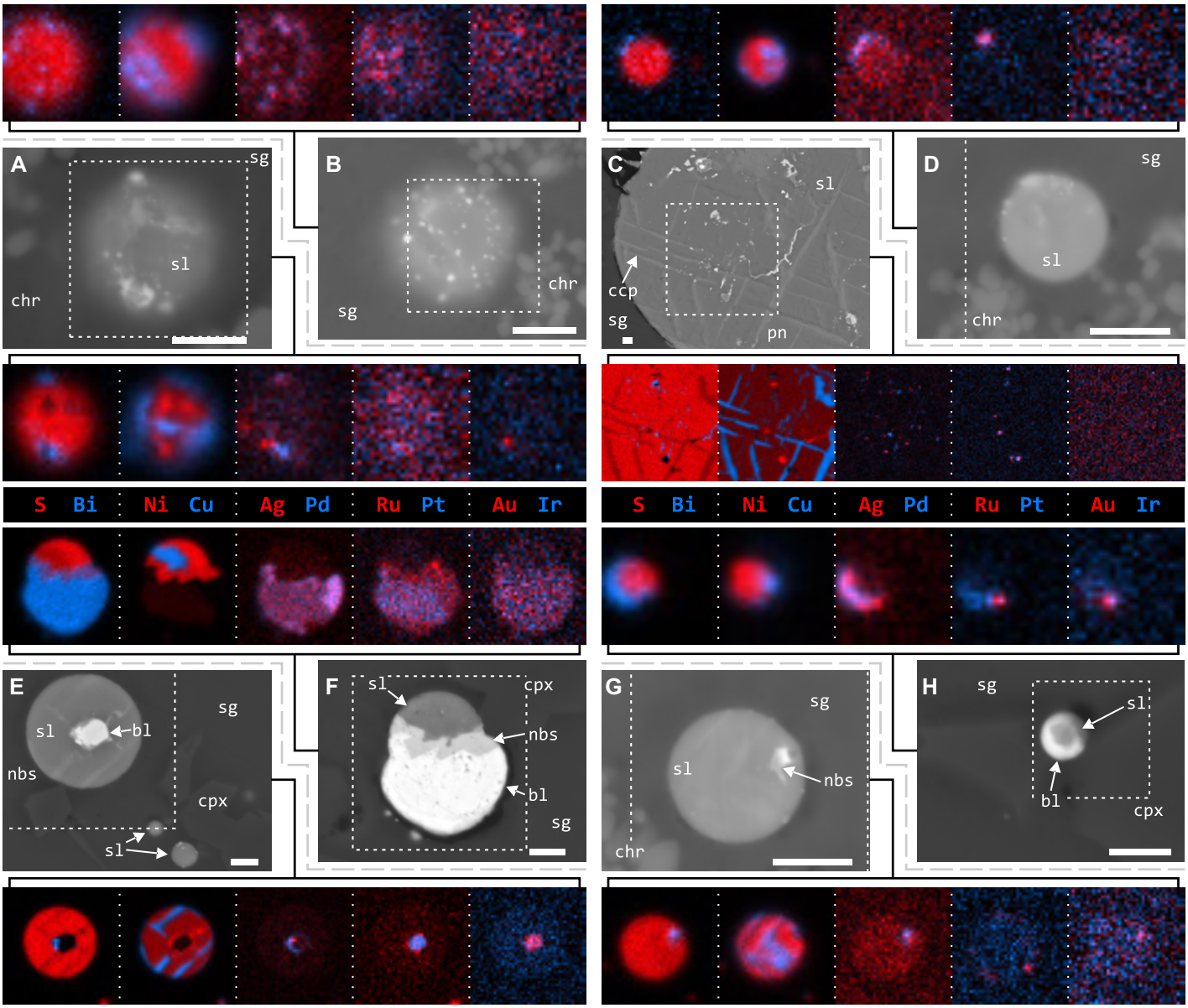

Figure 1. Electron probe microanalyzer (EPMA) images of products from run C5774. Grayscale images are backscattered electron (BSE) images, with corresponding X-ray element maps indicated by arrows from respective BSE images. Each map consists of two elements, with red or blue color indicated by legend strip. Dashed boxes and lines denote area shown in wavelength-dispersive spectroscopy maps. Scale bars are 1 µm. Abbreviations: bl—bismuthide liquid; ccp—chalcopyrite; chr—chromite; cpx—clinopyroxene; nbs—nickel bismuth sulfide; pn—pentlandite; sg—silicate glass; sl—quenched sulfide liquid. A high-resolution version of the figure is available in the Supplemental Material (see footnote 1).

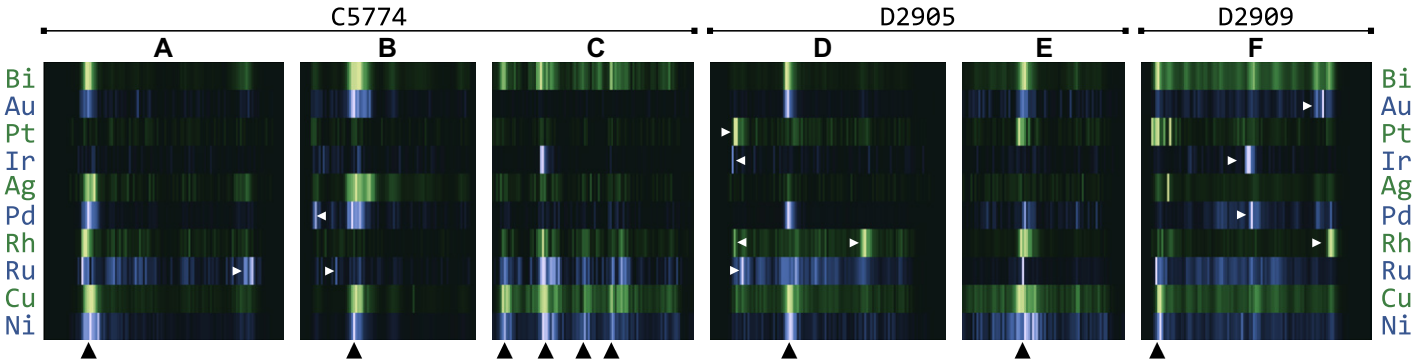

Figure 2. Semiquantitative down-laser-hole laser ablation–inductively coupled plasma–mass spectrometry (LA-ICP-MS) signal of silicate glass with noble metal (NM) nanonuggets and sulfide droplets. Representative plots are produced by normalizing element raw count data for each row to maximum color intensity. Each analysis represents 15–20 µm of hole depth. Colors alternate between blue and green for readability. Black arrows show individual sulfide droplets, and white arrows show NM phases not hosted by sulfide. Labels on top show which experiment each analysis is from. Each distinct vertical band represents time slice of ~660 ms. See the Supplemental Material (see footnote 1) for a high-resolution version of the figure and the full data set and data processing script in R programming language.

DISCUSSION

Solidified sulfide textures are invariably difficult to interpret because sulfide liquids do not quench to homogenous glass. Various flame-like textures are undoubtedly of quench origin and represent components dissolved in the sulfide liquid. The solidified sulfide droplets consist primarily of intergrown pentlandite (approximately $Ni_5Fe_4S_9$) and chalcopyrite ($CuFeS_2$) that formed on quench. Other than Fe, Cu, and Ni, the only other elements that show unequivocal quench textures are Ag and Bi, evident by their occurrence in flame textures (e.g., Fig. 1C), indicating their chalcophile character and higher solubility in sulfide liquids relative to the PGEs and Au (consistent with the natural observations of Holwell et al. [2015]). In contrast, the PGEs, Au, and some Ag occur as nanoscale nuggets on sulfide rims (Figs. 1A, 1B, and 1D) or as irregular patches within sulfides (Figs. 1E and 1G). It is difficult to envision a mechanism by which all NMs presumed dissolved in the sulfide liquid would migrate to droplet edges during quench and crystallize as nanonuggets protruding into the surrounding viscous silicate melt. Additionally, the lack of NM flame textures within pentlandite-chalcopyrite intergrowths argues against their solubility in the sulfide liquid, even when NMs constitute a significant proportion of a given droplet. If NMs were dissolved in the sulfide liquid, one would expect them to form flame textures as well, but such textures are not observed. When immiscible sulfide and bismuthide liquids coexist, some reaction is evident between the two separate phases during quench by the formation of Ni-Bi sulfides (Fig. 1F). These Ni-Bi sulfides are ubiquitous around NM patches within sulfide, suggesting that discrete NM-bismuthide droplets were present as immiscible liquids inside larger sulfide liquids at high temperature, instead of the NMs being dissolved within the sulfide phase (e.g., Figs. 1F and 1G). It is tempting to interpret the PGE phases as formed via exsolution from a single high-temperature homogenous sulfide phase; however, because the sulfide droplets are smaller than the laser spot (<2 µm versus 13 µm, respectively), the entire NM budget of each droplet is sampled and shown in Figure 2. Evidently, the composition and distribution of NMs vary between individual sulfide droplets. Had the NMs partitioned into sulfide liquid in equilibrium, all droplets (vertical bars marked by black arrows in Fig. 2) should contain similar NM contents. The variation shows that equilibrium partitioning has not occurred.

There are two aspects of equilibrium-disequilibrium relations demonstrated in our experiments. First, sulfide and bismuthide liquids equilibrate in seconds, with no kinetic barriers. The presence of NM nanonuggets on sulfide exteriors is therefore not the result of the nuggets lacking the time to dissolve in the sulfide, but is instead a result of real two-phase separation. Likewise, the sulfide-bismuthide immiscibility occurred because had it not, they would have dissolved in each other during the hours-long experiments. Second, the presence of isolated nanonuggets and differing PGE budgets of composite sulfide-bismuthide liquids within the silicate glass suggest that the silicate liquid forms a barrier to equilibrium. The diffusion coefficients of the NMs in silicate melts are unknown, but previous studies qualitatively demonstrated significant diffusion of silicate-dissolved NMs over hundreds of micrometers in as little as 10 min at comparable pressures and temperatures (Anenburg and Mavrogenes, 2016). However, once in metallic form, NM nanonuggets show exceptional resistance to dissolution over several hours (Anenburg and Mavrogenes, 2016). The equilibrium model dictates that silicate melts do not form a barrier for NM diffusion, but the presence of NM nanonuggets that are near but not touching sulfides or bismuthides in our experiments (white arrows in Fig. 2) argues otherwise. It is becoming clear that NM-rich layered intrusions form by hot magma pulses with a duration of only several years (Hepworth et al., 2020), and volcanic processes are usually only weeks long. Therefore, the exceptionally long time frames presumably required to achieve NM-silicate equilibrium may be rare in nature.

Notwithstanding sulfide-NM phase immiscibility, it is clear that the two are spatially associated. The NM nanonuggets and bismuthide liquids are mostly attached to or within sulfide liquids, exhibiting their tendency to agglomerate, when immersed in silicate liquid. Therefore, we suggest that the sulfide-NM association in nature is not primarily due to equilibrium chemical partitioning, but may occur due to mechanical entrapment (as suggested by Wirth et al. [2013] and González-Jiménez et al. [2019]). Thus, when sulfide liquids are in close proximity to NM nanonuggets and TABS melts (generalizing from the bismuthide liquids observed in our experiments), they coalesce within a dynamic silicate-dominated system. Because these natural systems contain orders of magnitude more sulfide liquid than NMs, probability dictates that the majority of NMs would be collected by sulfides, but it is still a matter of chance. Sulfide liquids, therefore, inherit the preexisting NM contents of their host silicate melts (e.g., González-Jiménez et al., 2019; Kamenetsky and Zelenski, 2020). This explains the sulfide-NM association, but does not preclude the presence of NM phases in silicate melts in the absence of sulfide.

Liquid immiscibility between sulfide and TABS liquids has been demonstrated in synthetic silica-free systems (Helmy et al., 2007, 2013; Helmy and Fonseca, 2017; Sinyakova et al., 2019; Helmy and Botcharnikov, 2020), but those experiments contained percentage levels of NMs and TABS, which highlighted immiscibility textures. In contrast, NM solubility and partitioning experiments are commonly conducted with much lower NM contents. In such experiments, NM nanonuggets are excluded when accounting for the NM contents of the

silicate glasses (Médard et al., 2015). Conversely, NMs are assumed to have been dissolved within the sulfide liquid while molten, and therefore included in the sulfide fraction. We suggest that this assumption is not founded, and that sulfide liquids are likewise contaminated with mechanically included NM nanonuggets, leading to spuriously high values. This, in turn, leads to an overestimation of sulfide-silicate partition coefficients, which are probably much lower than the reported values of as high as $n \times 10^6$ (Laurenz et al., 2016; Mungall and Brenan, 2014).

The presence of NM nanonuggets in silicate melts independent of sulfide melts potentially changes the way we view Earth's metal budget. Existing models of PGE deposit formation require extremely large volumes of silicate melt from which the PGEs are extracted and partitioned into a volumetrically small sulfide fraction (Naldrett et al., 2009). However, evidence for such voluminous melts is commonly lacking in the field (Holwell et al., 2015). The sulfur-poor characters of the Bushveld Complex–hosted Merensky Reef and UG-2 (South Africa) and other deposits (Naldrett et al., 2009; Holwell et al., 2015) may well be a primary feature of oxide-associated nanonugget accumulation. In the mantle, NMs are not necessarily associated with sulfides (Lorand and Luguet, 2016). During partial melting, NM nanonuggets can be entrained in rising silicate melts, evident by their presence inside silicate glasses or minerals (González-Jiménez et al., 2019; Ballhaus and Sylvester, 2000). The NM budget of such melts may be dominated by the nanonugget phase and not equilibrium solubility in the silicate liquid (Anenburg and Mavrogenes, 2016). In such cases, sulfide liquids play the secondary role of PGE entrapment and localized accumulation, whereas the initial PGE enrichment resulted from deeper silicate melting processes (e.g., Savelyev et al., 2018).

The presence of sulfide is a red herring that leads us to the misconception that sulfide liquid partitioning is a prerequisite for PGE deposit formation. This misconception requires all exploration models to include immense volumes of sulfide-saturated silicate melt and leads to all non-sulfide-associated PGE deposits being overlooked (Maier et al., 2003; Sá et al., 2005; Yang et al., 2018).

ACKNOWLEDGMENTS

Jeff Chen of the Centre for Advanced Microscopy (Microscopy Australia node at Australian National University [ANU]) assisted with electron probe microanalyzer (EPMA) analyses. Bei Chen of the Research School of Earth Sciences (ANU) assisted with laser ablation–inductively coupled plasma–mass spectrometry (LA-ICP-MS) analyses. We thank Vadim Kamenetsky, Katy Evans, and José María González-Jiménez for helpful comments.

REFERENCES CITED

Anenburg, M., and Mavrogenes, J.A., 2016, Experimental observations on noble metal nanonuggets and Fe-Ti oxides, and the transport of platinum group elements in silicate melts: Geochimica et Cosmochimica Acta, v. 192, p. 258–278, https://doi.org/10.1016/j.gca.2016.08.010.

Ballhaus, C., and Sylvester, P., 2000, Noble metal enrichment processes in the Merensky Reef, Bushveld Complex: Journal of Petrology, v. 41, p. 545–561, https://doi.org/10.1093/petrology/41.4.545.

Barnes, S.-J., and Ripley, E.M., 2016, Highly siderophile and strongly chalcophile elements in magmatic ore deposits: Reviews in Mineralogy and Geochemistry, v. 81, p. 725–774, https://doi.org/10.2138/rmg.2016.81.12.

Campbell, I.H., and Naldrett, A.J., 1979, The influence of silicate:sulfide ratios on the geochemistry of magmatic sulfides: Economic Geology and the Bulletin of the Society of Economic Geologists, v. 74, p. 1503–1506, https://doi.org/10.2113/gsecongeo.74.6.1503.

Day, J.M.D., Brandon, A.D., and Walker, R.J., 2016, Highly siderophile elements in Earth, Mars, the Moon, and asteroids: Reviews in Mineralogy and Geochemistry, v. 81, p. 161–238, https://doi.org/10.2138/rmg.2016.81.04.

Finnigan, C.S., Brenan, J.M., Mungall, J.E., and McDonough, W.F., 2008, Experiments and models bearing on the role of chromite as a collector of platinum group minerals by local reduction: Journal of Petrology, v. 49, p. 1647–1665, https://doi.org/10.1093/petrology/egn041.

Godel, B., 2015, Platinum-group element deposits in layered intrusions: Recent advances in the understanding of the ore forming processes, *in* Charlier, B., et al., eds., Layered Intrusions: Dordrecht, Springer, p. 379–432, https://doi.org/10.1007/978-94-017-9652-1_9.

Godel, B., Barnes, S.J., Barnes, S.-J., and Maier, W.D., 2010, Platinum ore in three dimensions: Insights from high-resolution X-ray computed tomography: Geology, v. 38, p. 1127–1130, https://doi.org/10.1130/G31265.1.

González-Jiménez, J.M., et al., 2019, Magmatic platinum nanoparticles in metasomatic silicate glasses and sulfides from Patagonian mantle xenoliths: Contributions to Mineralogy and Petrology, v. 174, 47, https://doi.org/10.1007/s00410-019-1583-5.

Gunn, G., 2014, Platinum-group metals, *in* Gunn, G., ed., Critical Metals Handbook: Chichester, UK, John Wiley & Sons, p. 284–311, https://doi.org/10.1002/9781118755341.ch12.

Helmy, H.M., and Botcharnikov, R., 2020, Experimental determination of the phase relations of Pt and Pd antimonides and bismuthinides in the Fe-Ni-Cu sulfide systems between 1100 and 700 °C: The American Mineralogist, v. 105, p. 344–352, https://doi.org/10.2138/am-2020-7154.

Helmy, H.M., and Fonseca, R.O.C., 2017, The behavior of Pt, Pd, Cu and Ni in the Se-sulfide system between 1050 and 700 °C and the role of Se in platinum-group elements fractionation in sulfide melts: Geochimica et Cosmochimica Acta, v. 216, p. 141–152, https://doi.org/10.1016/j.gca.2017.05.010.

Helmy, H.M., Ballhaus, C., Berndt, J., Bockrath, C., and Wohlgemuth-Ueberwasser, C., 2007, Formation of Pt, Pd and Ni tellurides: Experiments in sulfide–telluride systems: Contributions to Mineralogy and Petrology, v. 153, p. 577–591, https://doi.org/10.1007/s00410-006-0163-7.

Helmy, H.M., Ballhaus, C., Fonseca, R.O.C., and Nagel, T.J., 2013, Fractionation of platinum, palladium, nickel, and copper in sulfide–arsenide systems at magmatic temperature: Contributions to Mineralogy and Petrology, v. 166, p. 1725–1737, https://doi.org/10.1007/s00410-013-0951-9.

Hepworth, L.N., Daly, J.S., Gertisser, R., Johnson, C.G., Emeleus, C.H., and O'Driscoll, B., 2020, Rapid crystallization of precious-metal-mineralized layers in mafic magmatic systems: Nature Geoscience, v. 13, p. 375–381, https://doi.org/10.1038/s41561-020-0568-3.

Holwell, D.A., and McDonald, I., 2010, A review of the behaviour of platinum group elements within natural magmatic sulfide ore systems: Platinum Metals Review, v. 54, p. 26–36, https://doi.org/10.1595/147106709X480913.

Holwell, D.A., Keays, R.R., McDonald, I., and Williams, M.R., 2015, Extreme enrichment of Se, Te, PGE and Au in Cu sulfide microdroplets: Evidence from LA-ICP-MS analysis of sulfides in the Skaergaard Intrusion, east Greenland: Contributions to Mineralogy and Petrology, v. 170, 53, https://doi.org/10.1007/s00410-015-1203-y.

Kamenetsky, V.S., and Zelenski, M., 2020, Origin of noble-metal nuggets in sulfide-saturated arc magmas: A case study of olivine-hosted sulfide melt inclusions from the Tolbachik volcano (Kamchatka, Russia): Geology, v. 48, p. 620–624, https://doi.org/10.1130/G47086.1.

Kawohl, A., and Frimmel, H.E., 2016, Isoferroplatinum-pyrrhotite-troilite intergrowth as evidence of desulfurization in the Merensky Reef at Rustenburg (western Bushveld Complex, South Africa): Mineralogical Magazine, v. 80, p. 1041–1053, https://doi.org/10.1180/minmag.2016.080.055.

Laurenz, V., Rubie, D.C., Frost, D.J., and Vogel, A.K., 2016, The importance of sulfur for the behavior of highly-siderophile elements during Earth's differentiation: Geochimica et Cosmochimica Acta, v. 194, p. 123–138, https://doi.org/10.1016/j.gca.2016.08.012.

Lorand, J.-P., and Luguet, A., 2016, Chalcophile and siderophile elements in mantle rocks: Trace elements controlled by trace minerals: Reviews in Mineralogy and Geochemistry, v. 81, p. 441–488, https://doi.org/10.2138/rmg.2016.81.08.

Luguet, A., and Reisberg, L., 2016, Highly siderophile element and ^{187}Os signatures in non-cratonic basalt-hosted peridotite xenoliths: Unravelling the origin and evolution of the post-Archean lithospheric mantle: Reviews in Mineralogy and Geochemistry, v. 81, p. 305–367, https://doi.org/10.2138/rmg.2016.81.06.

Maier, W.D., Barnes, S.-J., Gartz, V., and Andrews, G., 2003, Pt-Pd reefs in magnetitites of the Stella layered intrusion, South Africa: A world of new exploration opportunities for platinum group elements: Geology, v. 31, p. 885–888, https://doi.org/10.1130/G19746.1.

Maier, W.D., Rasmussen, B., Fletcher, I.R., Godel, B., Barnes, S.J., Fisher, L.A., Yang, S.H., Huhma, H., and Lahaye, Y., 2015, Petrogenesis of the ~2.77 Ga Monts de Cristal Complex, Gabon: Evidence for direct precipitation of Pt-arsenides from basaltic magma: Journal of Petrology, v. 56, p. 1285–1308, https://doi.org/10.1093/petrology/egv035.

Médard, E., Schmidt, M.W., Wälle, M., Keller, N.S., and Günther, D., 2015, Platinum partitioning between metal and silicate melts: Core formation, late veneer and the nanonuggets issue: Geochimica et Cosmochimica Acta, v. 162, p. 183–201, https://doi.org/10.1016/j.gca.2015.04.019.

Mungall, J.E., and Brenan, J.M., 2014, Partitioning of platinum-group elements and Au between sulfide liquid and basalt and the origins of mantle-crust fractionation of the chalcophile elements: Geochimica et Cosmochimica Acta, v. 125, p. 265–289, https://doi.org/10.1016/j.gca.2013.10.002.

Naldrett, A.J., Wilson, A., Kinnaird, J., and Chunnett, G., 2009, PGE tenor and metal ratios within and below the Merensky Reef, Bushveld Complex: Implications for its genesis: Journal of Petrology, v. 50, p. 625–659, https://doi.org/10.1093/petrology/egp015.

Sá, J.H.S., Barnes, S.-J., Prichard, H.M., and Fisher, P.C., 2005, The distribution of base metals and platinum-group elements in magnetitite and its host rocks in the Rio Jacaré intrusion, northeastern Brazil: Economic Geology and the Bulletin of the Society of Economic Geologists, v. 100, p. 333–348, https://doi.org/10.2113/gsecongeo.100.2.333.

Sattari, P., Brenan, J.M., Horn, I., and McDonough, W.F., 2002, Experimental constraints on the sulfide- and chromite-silicate melt partitioning behavior of rhenium and platinum-group elements: Economic Geology and the Bulletin of the Society of Economic Geologists, v. 97, p. 385–398, https://doi.org/10.2113/gsecongeo.97.2.385.

Savelyev, D.P., et al., 2018, Immiscible sulfide melts in primitive oceanic magmas: Evidence and implications from picrite lavas (Eastern Kamchatka, Russia): The American Mineralogist, v. 103, p. 886–898, https://doi.org/10.2138/am-2018-6352.

Sinyakova, E.F., Kosyakov, V.I., and Goryachev, N.A., 2019, Formation of drop-shaped inclusions based on Pt, Pd, Au, Ag, Bi, Sb, Te, and As under crystallization of an intermediate solid solution in the Cu–Fe–Ni–S system: Doklady Earth Sciences, v. 489, p. 1301–1305, https://doi.org/10.1134/S1028334X19110072.

Spandler, C.J., Eggins, S.M., Arculus, R.J., and Mavrogenes, J.A., 2000, Using melt inclusions to determine parent-magma compositions of layered intrusions: Application to the Greenhills Complex (New Zealand), a platinum group minerals–bearing, island-arc intrusion: Geology, v. 28, p. 991–994, https://doi.org/10.1130/0091-7613(2000)28<991:UMITDP>2.0.CO;2.

Wirth, R., Reid, D., and Schreiber, A., 2013, Nanometer-sized platinum-group minerals (PGM) in base metal sulfides: New evidence for an orthomagmatic origin of the Merensky Reef PGE ore deposit, Bushveld Complex, South Africa: The Canadian Mineralogist, v. 51, p. 143–155, https://doi.org/10.3749/canmin.51.1.143.

Yang, S.-H., Su, B.-X., Huang, X.-W., Tang, D.-M., Qin, K.-Z., Bai, Y., Sakyi, P.A., and Alemayehu, M., 2018, Platinum-group mineral occurrences and platinum-group elemental geochemistry of the Xiadong Alaskan-type complex in the southern Central Asian Orogenic Belt: Minerals (Basel), v. 8, p. 494, https://doi.org/10.3390/min8110494.

Zelenski, M., Kamenetsky, V.S., Mavrogenes, J.A., Danyushevsky, L.V., Matveev, D., and Gurenko, A.A., 2017, Platinum-group elements and gold in sulfide melts from modern arc basalt (Tolbachik volcano, Kamchatka): Lithos, v. 290–291, p. 172–188, https://doi.org/10.1016/j.lithos.2017.08.012.

Printed in USA